



## NONPOLYNOMIAL CUBIC SPLINE APPROXIMATION FOR THE EQUAL WIDTH EQUATION

ALI SAHIN AND LEVENT AKYUZ

**ABSTRACT.** In this paper, we investigate the numerical solutions of the equal width (EW) equation via the nonpolynomial cubic spline functions. Crank-Nicolson formulas are used for time discretization of the target equation. A linearization technique is also employed for the numerical purpose. Accuracy of the method is observed by the pointwise rate of convergence. Stability of the suggested method is investigated via the von-Neumann analysis. Six numerical examples related to single solitary wave, interaction of two, three and opposite waves, wave undulation and the Maxwell wave are considered as the test problems. The accuracy and the efficiency of the purposed method are measured by  $L_\infty$  and  $L_2$  error norms and conserved constants. The obtained results are compared with the possible analytical values and those in some earlier studies.

### 1. INTRODUCTION

The field of nonlinear dispersive waves is one of the rapidly developed area in science over the last few decades. Because of their attractive solutions such as shallow water and plasma waves, studying on this field has been source of interest. Since the analytical solutions are not available in general and the possible cases are limited, numerical solutions for those equations have importance to understand the nonlinear phenomena.

There are many different models for the nonlinear dispersive waves in the literature. In this paper, we focus on the equal width (EW) equation which is first suggested by Morrison et.al. [2] and it represents an alternative to the well known KdV and RLW equations.

The EW equation has the following form:

$$(1.1) \quad \frac{\partial u}{\partial t} + u \frac{\partial u}{\partial x} - \mu \frac{\partial^3 u}{\partial x^2 \partial t} = 0$$

---

*Date:* May 19, 2015 and, in revised form, September 2, 2015.

*2000 Mathematics Subject Classification.* 35Q51; 35Q53; 41A15.

*Key words and phrases.* EW equation; Nonpolynomial spline; Solitary waves.

where  $\mu$  is a positive parameter and  $u$  is a smooth function that represents the wave amplitude on a domain  $\Omega \times [0, T]$  with  $\Omega \in \mathbb{R}$ . The only possible analytical solution of Eq.(1.1) is the single travelling solitary wave solution. Therefore numerical methods have to be used for some other initial conditions such as interactions, undulation or the Maxwell initial condition.

Numerical methods including spectral method[4], least squares finite element method[5], Galerkin method[6][8][9], collocation method[7][10][14], finite difference method[12][13], differential quadrature method, meshless method[14][22] and Petrov-Galerkin method[3][19] have been presented in the literature for the EW equation.

Spline approximation is based upon to divide the solution domain into a collection of subdomains and construct an approximating function on each subdomains. The most known spline approximation is the cubic spline in which piecewise cubic polynomials are used for the approximation. The objective of spline approximation is to obtain an interpolation formula that has continuous derivatives in required order both within the intervals and at the interpolating nodes.

Nonpolynomial spline based methods have been used for some other partial differential equations such as non-linear Schrödinger equation[20], RLW equation[21], Burgers' equation[16], Klein-Gordon equation[17], Bratu's problem[18]. However, with our knowledge, numerical solution of the EW equation has not been published yet. The aim of this paper is to investigate the numerical solution of the EW equation via the nonpolynomial cubic spline method. Crank-Nicolson method and Rubin-Graves technique[1] are also used for the time discretization and the linearization of the governing equation respectively.

This paper is organized as follows: Section 2 is devoted to the numerical method. Truncation error and stability analysis are also given in that section. The numerical testing and the comparisons on the examples are studied in Section 3. Finally, a conclusion is presented in the last section.

## 2. NUMERICAL METHOD

Let's start the numerical method by partitioning the solution domain  $\Omega \in \mathbb{R}$  into subintervals. For this purpose, we consider  $N + 1$  equally distributed mesh points such that

$$\Omega : x_0 < x_1 < \dots < x_N$$

where  $x_{i+1} = x_i + h$ ,  $i = 0, 1, \dots, N - 1$  and  $h$  is the grid size.

The proposed spline functions in this paper have the form

$$T_3 = \text{span}\{1, x, \sin(\omega x), \cos(\omega x)\}$$

where  $\omega$  is the frequency of the trigonometric part of the spline. The cubic non-polynomial spline functions can be constructed over this mesh as follows:

$$(2.1) \quad \begin{aligned} P_i(x, t_j) = & a_i(t_j) \cos[\omega(x - x_i)] + b_i(t_j) \sin[\omega(x - x_i)] \\ & + c_i(t_j)(x - x_i) + d_i(t_j) \end{aligned}$$

where  $i$  and  $j$  are indices for space and time respectively.

Because of the spline properties, it can written that

$$U_i^j = P_i(x_i, t_j), \quad U_{i+1}^j = P_i(x_{i+1}, t_j),$$

$$S_i^j = P_i''(x_i, t_j), \quad S_{i+1}^j = P_i''(x_{i+1}, t_j).$$

Then the coefficients in Eq.(2.1) are obtained as

$$a_i = -\frac{h^2}{\theta^2} S_i^j, \quad b_i = \frac{h^2 (S_i^j \cos \theta - S_{i+1}^j)}{\theta^2 \sin \theta},$$

$$c_i = \frac{U_{i+1}^j - U_i^j}{h} + \frac{h (S_{i+1}^j - S_i^j)}{\theta^2}, \quad d_i = \frac{h^2}{\theta^2} S_i^j + U_i^j$$

where  $\theta = \omega h$  and capital  $U$  is used for the approximation to the exact function  $u$ .

Another useful tool for the purposed method comes from the continuity of the first derivatives. Having first order continuous derivatives at grid points, i.e.  $P_i'(x_i, t_j) = P_{i-1}'(x_i, t_j)$ , gives the equation

$$(2.2) \quad b_i \omega + c_i = -a_{i-1} \omega \sin \theta + b_{i-1} \omega \cos \theta + c_{i-1}.$$

Substitution of related coefficients in Eq.(2.2) and slight arrangements on it lead to the following relation between the solutions and their second derivatives:

$$(2.3) \quad U_{i-1}^j - 2U_i^j + U_{i+1}^j = \alpha S_{i-1}^j + \beta S_i^j + \alpha S_{i+1}^j, \quad i = 1, 2, \dots, N-1$$

where  $\alpha = \frac{h^2}{\theta \sin \theta} - \frac{h^2}{\theta^2}$  and  $\beta = -\frac{2h^2 \cos \theta}{\theta \sin \theta} + \frac{2h^2}{\theta^2}$ . Also note here that if  $\theta \rightarrow 0$  then  $\alpha \rightarrow \frac{h^2}{6}$  and  $\beta \rightarrow \frac{2h^2}{3}$  which means the standard cubic spline case.

Eq.(2.3) can be written between two successive time levels  $j$  and  $j+1$  so that

$$(2.4) \quad \begin{aligned} & (U_{i-1}^{j+1} - U_{i-1}^j) - 2(U_i^{j+1} - U_i^j) + (U_{i+1}^{j+1} - U_{i+1}^j) = \\ & \alpha (S_{i-1}^{j+1} - S_{i-1}^j) + \beta (S_i^{j+1} - S_i^j) + \alpha (S_{i+1}^{j+1} - S_{i+1}^j) \end{aligned}$$

where  $i = 1, 2, \dots, N-1$ . The present numerical method will be built on Eq.(2.4).

**Theorem 2.1.** *The difference equation (2.4) has the local truncation error of order*

- i)  $O(h^2)$  when  $2\alpha + \beta \neq h^2$ ,
- ii)  $O(h^4)$  when  $2\alpha + \beta = h^2$  and  $\alpha \neq h^2/12$ ,
- iii)  $O(h^6)$  when  $2\alpha + \beta = h^2$  and  $\alpha = h^2/12$ .

*Proof.* It was proved in [21] by using the Taylor series expansion, see [21].  $\square$

Besides the spline relation (2.4), the EW equation gives some additional facts about the second derivative of the solution. First, Eq.(1.1) may be rearranged as

$$\frac{\partial}{\partial t} \left( \frac{\partial^2 u}{\partial x^2} - \frac{1}{\mu} u \right) = \frac{1}{\mu} \left( u \frac{\partial u}{\partial x} \right).$$

Then following Crank-Nicolson scheme for the time discretization, the EW equation turns into the form:

$$(2.5) \quad \left[ \frac{\partial^2 U}{\partial x^2} - \frac{1}{\mu} U \right]_{x=x_i}^{t=t_{j+1}} - \left[ \frac{\partial^2 U}{\partial x^2} - \frac{1}{\mu} U \right]_{x=x_i}^{t=t_j} = \frac{k}{2\mu} \left( \left[ U \frac{\partial U}{\partial x} \right]_{x=x_i}^{t=t_{j+1}} + \left[ U \frac{\partial U}{\partial x} \right]_{x=x_i}^{t=t_j} \right)$$

The nonlinear term in Eq.(2.5) can be linearized with the technique

$$(UU_x)^{j+1} = U^{j+1} U_x^j + U^j U_x^{j+1} - U^j U_x^j$$

which is suggested by Rubin and Graves[1] as

$$(2.6) \quad S^{j+1} - S^j = \frac{1}{\mu} (U^{j+1} - U^j) + \frac{k}{2\mu} (U^{j+1}U_x^j + U^jU_x^{j+1}).$$

Using difference formulas for the first order space derivatives in Eq.(2.6) leads to

$$(2.7) \quad \begin{cases} S_{i-1}^{j+1} - S_{i-1}^j = \frac{1}{\mu} (U_{i-1}^{j+1} - U_{i-1}^j) + 2rU_{i-1}^{j+1} (U_i^j - U_{i-1}^j) + 2rU_{i-1}^j (U_i^{j+1} - U_{i-1}^{j+1}), \\ S_i^{j+1} - S_i^j = \frac{1}{\mu} (U_i^{j+1} - U_i^j) + rU_i^{j+1} (U_{i+1}^j - U_{i-1}^j) + rU_i^j (U_{i+1}^{j+1} - U_{i-1}^{j+1}), \\ S_{i+1}^{j+1} - S_{i+1}^j = \frac{1}{\mu} (U_{i+1}^{j+1} - U_{i+1}^j) + 2rU_{i+1}^{j+1} (U_{i+1}^j - U_i^j) + 2rU_{i+1}^j (U_{i+1}^{j+1} - U_i^{j+1}) \end{cases}$$

where  $r = k/(4\mu h)$ .

Finally, considering Eq.(2.4) together with Eq.(2.7) gives the recurrence relation

$$(2.8) \quad A_i U_{i-1}^{j+1} + B_i U_i^{j+1} + C_i U_{i+1}^{j+1} = D_i U_{i-1}^j + E_i U_i^j + F_i U_{i+1}^j$$

where

$$A_i = 1 - \alpha/\mu + 4\alpha r U_{i-1}^j - r(2\alpha - \beta) U_i^j,$$

$$B_i = -2 - \beta/\mu + r(2\alpha - \beta) (U_{i+1}^j - U_{i-1}^j),$$

$$C_i = 1 - \alpha/\mu - 4\alpha r U_{i+1}^j + r(2\alpha - \beta) U_i^j,$$

$$D_i = 1 - \alpha/\mu,$$

$$E_i = -2 - \beta/\mu,$$

$$F_i = 1 - \alpha/\mu.$$

The recurrence relation (2.8) contains  $N - 1$  equations in  $N + 1$  unknowns. By adding two equations from the boundary conditions, it will be a solvable linear system. After the initial solutions  $U^0$  computed from the initial condition, all the other solutions at different time levels are calculated from the system (2.8).

**2.1. Stability analysis.** According to von-Neumann analysis, it is assumed that the solution of the governing equation is in the following form:

$$U_i^j = \xi^j e^{q\varphi i h}$$

where  $q$  is the imaginary unit,  $\varphi$  is the wave number and  $\xi$  is the amplification factor. Substitution of the above expression in Eq.(2.8) yields

$$\begin{aligned} & A_i \xi^{j+1} e^{q\varphi(i-1)h} + B_i \xi^{j+1} e^{q\varphi i h} + C_i \xi^{j+1} e^{q\varphi(i+1)h} \\ &= D_i \xi^j e^{q\varphi(i-1)h} + E_i \xi^j e^{q\varphi i h} + F_i \xi^j e^{q\varphi(i+1)h}. \end{aligned}$$

Then

$$\xi = \frac{\left(2 - \frac{2\alpha}{\mu}\right) \cos \varphi h - 2 - \frac{\beta}{\mu} + q(2\alpha + \beta) 2rd^*}{\left(2 - \frac{2\alpha}{\mu}\right) \cos \varphi h - 2 - \frac{\beta}{\mu} - q(2\alpha + \beta) 2rd^*}$$

where  $d^*$  is locally constant for  $U$  in the nonlinear terms. Hence, the above expression gives  $|\xi| = 1$  which means that the numerical method is unconditionally stable.

### 3. TEST PROBLEMS

In this section, several test problems take part in order to show the accuracy and the efficiency of the numerical method. The accuracy is measured by  $L_\infty$  and  $L_2$  error norms that are defined by

$$L_\infty = \max_i |u_i^{exact} - U_i^{numeric}|,$$

$$L_2 = \sqrt{h \sum_{i=0}^N |u_i^{exact} - U_i^{numeric}|^2}.$$

In all numerical computations except the motion of single solitary wave, the discretization parameters are chosen as  $h = 0.1$  and  $k = 0.1$ . Additionally, similar to the reference [21], the parameters  $\alpha$  and  $\beta$  are selected as  $2\alpha + \beta = h^2$  and  $\alpha = h^2/4$  in all computations.

The EW equation has also the following conserved quantities:

$$C_1 = \int_a^b u dx, \quad C_2 = \int_a^b \left( u^2 + \mu (u_x)^2 \right) dx, \quad C_3 = \int_a^b u^3 dx$$

which correspond to mass, momentum and energy respectively. These invariants also give an idea about the accuracy of the numerical method especially in cases that the equation does not have an analytical solution. Therefore the invariants are monitored to check the conservation of the numerical algorithms for all test problems.

In order to compute the rate of convergence, the algorithm has been performed for difference space and time steps. Then the results are used in the formula

$$\text{space order} = \frac{\log(\|u - u_{h_i}\|_2 / \|u - u_{h_{i+1}}\|_2)}{\log(h_i/h_{i+1})}$$

$$\text{time order} = \frac{\log(\|u - u_{k_i}\|_2 / \|u - u_{k_{i+1}}\|_2)}{\log(k_i/k_{i+1})}$$

where  $u$  is the exact solution and  $u_{h_i}$  and  $u_{k_i}$  are the numerical solutions for space size  $h_i$  and time step  $k_i$  respectively.

**3.1. Motion of single solitary wave.** A single solitary wave which is initially centered at  $\tilde{x}_s$  and travels with a constant velocity has the following analytical solution

$$(3.1) \quad u(x, t) = 3c \operatorname{sech}^2 [K(x - \tilde{x}_s - ct)],$$

where  $K = 1/\sqrt{4\mu}$  is the width of the wave pulse,  $c$  is the velocity and  $3c$  is the magnitude of the wave.

The initial condition comes from Eq.(3.1) and the boundary conditions are given by

$$u(x_0, t) = 0 \quad \text{and} \quad u(x_N, t) = 0.$$

The common parameter choices in the literature are  $\mu = 1$  and  $x_s = 10$ . Although almost all earlier papers use same time increment, i.e.  $k = 0.05$ , there are some different considerations for the grid size. For instance,  $h = 0.15$  in [22] and MM[14],  $h = 0.1$  in DQM[14],  $h = 0.05$  in [7], [9] and [6]. In this test problem, similar to QBGM[14], the solutions are calculated over  $\Omega = [0, 30]$  and  $t \in [0, 80]$  with the discretization parameters  $h = 0.03$  and  $k = 0.05$ . The solution profiles are illustrated in Fig.1-2 for  $c = 0.1$  and Fig.3-4 for  $c = 0.03$  at different times. It is clear from these figures that solutions remain in same profile.

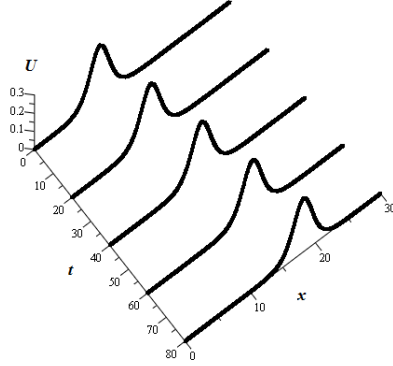


**Fig.1:** Solitary waves for  $c = 0.1$

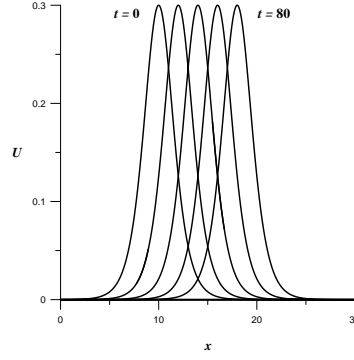


**Fig.2:** Solitary waves for  $c = 0.1$

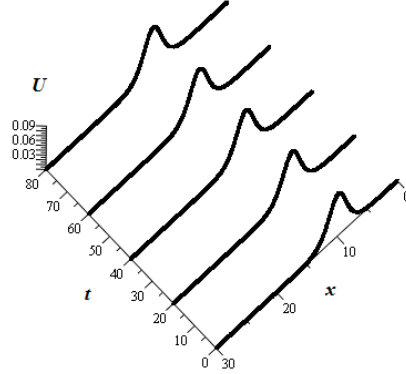


**Fig.3:** Solitary waves for  $c = 0.03$

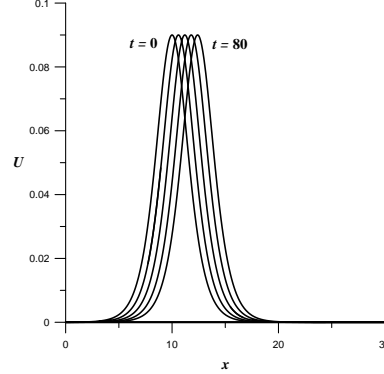


**Fig.4:** Solitary waves for  $c = 0.03$

The analytical values of the invariants are calculated by

$$C_1 = \frac{6c}{K}, \quad C_2 = \frac{12c^2}{K} + \frac{48Kc^2\mu}{5}, \quad C_3 = \frac{144c^3}{5K}$$

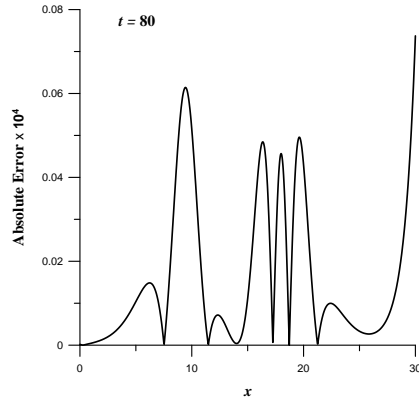
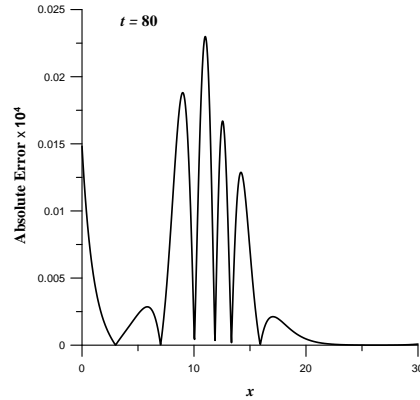
that correspond to  $C_1 = 1.2$ ,  $C_2 = 0.288$  and  $C_3 = 0.0576$  for  $c = 0.1$  and  $C_1 = 0.36$ ,  $C_2 = 0.02592$  and  $C_3 = 0.001555$  for  $c = 0.03$ . Computed errors and invariants are presented in Table 1 and Table 3 for  $c = 0.1$  and  $c = 0.03$  respectively. According to Table 1 and 3, the present results are acceptable and the given method is comparable with others.

**Table 1**

 Errors and invariants at time  $t = 80$  for  $c = 0.1$ 

Method	$L_\infty \times 10^4$	$L_2 \times 10^4$	$C_1$	$C_2$	$C_3$
Analytic			1.2	0.288	0.05760
Present	0.07372964	0.1289443	1.199985	0.2879897	0.05760
[7]	0.53	0.56	1.19998	0.28798	0.05759
[9]	0.21	0.29	1.19995	0.28798	0.05759
[6]	0.01704	0.03064	1.19999	0.28801	0.05760
QBGM[14]	0.07370	0.06095	1.20000	0.288000	0.05760
DQM[14]	0.07373	0.07035	1.19999	0.288000	0.05760
MM[14]	0.20296	0.31198	1.20003	0.288000	0.05760
W(7,5)[22]	0.03537611	0.03360406	1.19999752	0.28800001	0.05760

Absolute error distributions at  $t = 80$  are plotted in Fig.5 and Fig.6. Due to the relatively high velocity, the solution domain is short when  $c = 0.1$ . Therefore the maximum error is observed at the right hand boundary in Fig.5. To overcome this problem, the solution domain can be extended so that the error at the right hand boundary decreases.


**Fig.5:** Absolute error for  $c = 0.1$ 

**Fig.6:** Absolute error for  $c = 0.03$ 

The orders for pointwise rate of convergence are given in Table 2 which shows that the present method has second order accuracy in terms of both space and time.

**Table 2:** Rate of convergence

Spatial order ( $\Delta t = 0.05$ )		Temporal order ( $h = 0.03$ )	
$h_i$	$t = 80$	$\Delta t_i$	$t = 80$
2.00		2.00	
1.00	3.1914841	1.00	1.9942460
0.50	2.1804472	0.50	2.0091253
0.25	2.0403988	0.25	2.0364273
0.125	2.0157560	0.125	1.9910816
0.0625	2.0207153	0.0625	0.9043434

**Table 3**Errors and invariants at time  $t = 80$  for  $c = 0.03$ 

Method	$L_\infty \times 10^4$	$L_2 \times 10^4$	$C_1$	$C_2$	$C_3$
Analytic			0.36000	0.02592	0.001555
Present	0.02299	0.03812	0.359997	0.025919	0.0015552
[8]	18.36	26.83	0.36665	0.02658	
[9]	0.07	0.13	0.36000	0.02592	0.00156
[6]	0.01483	0.01025	0.36000	0.02592	0.00156
QBGM[14]	0.01483	0.01064	0.36000	0.02592	0.00156
DQM[14]	0.01483	0.00934	0.36000	0.02592	0.00156
MM[14]	0.07598	0.04911	0.36000	0.02592	0.00156
W(7,5)[22]	0.01418041	0.01267701	0.36000055	0.02592	0.0015552

**3.2. Interaction of two solitary waves.** As a second problem, interaction of two solitary waves is considered. The initial condition

$$(3.2) \quad \left. \begin{aligned} u_0(x) &= U_1 + U_2 \\ U_j &= 3c_j \operatorname{sech}^2[K_j(x - \tilde{x}_j - c_j)], \quad j = 1, 2 \end{aligned} \right\}$$

yields two waves travelling in same direction and having amplitude  $3c_1$  and  $3c_2$ . These waves are initially positioned at  $x = \tilde{x}_1$  and  $x = \tilde{x}_2$  respectively. The following parameter choices give a complete interaction over the solution domain  $x \in [0, 80]$ .

$$\mu = 1, \quad K_1 = 0.5, \quad K_2 = 0.5, \quad \tilde{x}_1 = 10, \quad \tilde{x}_2 = 25, \quad c_1 = 1.5, \quad c_2 = 0.75.$$

To illustrate the interaction, the solution profiles are figured in Fig.7-8 at three different times. The figures show that there is no decay on the solitary waves after the interaction. However, as seen in Fig.9, there are some changes on magnitudes for both waves at the interaction process.

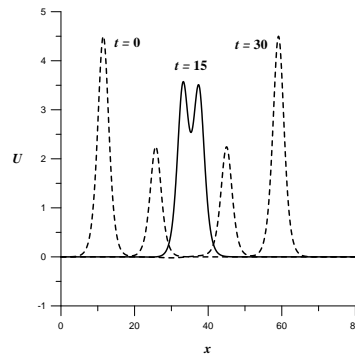
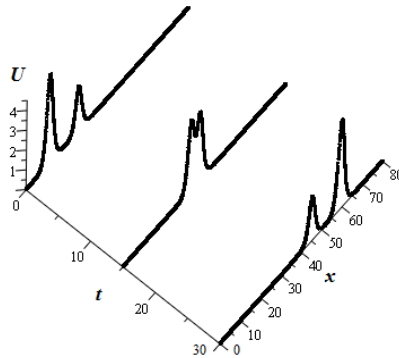


**Fig.7:** Interaction of two solitary waves    **Fig.8:** Interaction of two solitary waves

In order to see the results quantitatively and to make a comparison, Table 4 is constructed. Since there is no analytical solution with the considered initial

condition (3.2), only the invariants are compared in the table. Analytical values of the invariants are

$$C_1 = 12(c_1 + c_2) = 27, \quad C_2 = 28.8(c_1^2 + c_2^2) = 81, \quad C_3 = 57.6(c_1^3 + c_2^3) = 218.7.$$

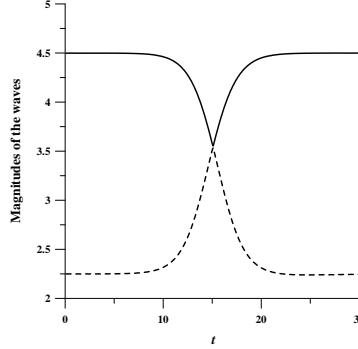


**Fig.9:** Magnitudes of the waves

**Table 4**

Invariants for the interaction of two solitary waves at  $t = 30$ .

Method	$C_1$	$C_2$	$C_3$
Analytic	27	81	218.7
Present	26.999997	80.968402	218.70289
[9]	27.00003	81.01719	218.70650
[6]	27.00068	81.02407	218.73673
[10]	27.12702	80.98988	218.6996
QBGm[14]	26.99973	80.99778	218.69094
DQM[14]	27.00017	81.00044	218.70304
MM[14]	27.00024	81.00140	218.70694
W(7,5)[22]	27.000049	81.000204	218.70186

**3.3. Interaction of three solitary waves.** Interaction of three solitary waves is figured out in this subsection. The initial condition

$$u_0(x) = \sum_{j=1}^3 3c_j \operatorname{sech}^2 [K_j(x - \tilde{x}_j - c_j)]$$

where

$$K_1 = K_2 = K_3 = 0.5, \quad c_1 = 4.5, \quad c_2 = 1.5, \quad c_3 = 0.5, \quad \tilde{x}_1 = 10, \quad \tilde{x}_2 = 25, \quad \tilde{x}_3 = 35$$

leads to three waves which interact together. Figs.10-11 shows the complete interaction. The backmost wave passes the others without any decay on its profile. The invariants are tabulated at  $t = 15$  for  $h = 0.1$  and  $k = 0.1$  in Table 5.

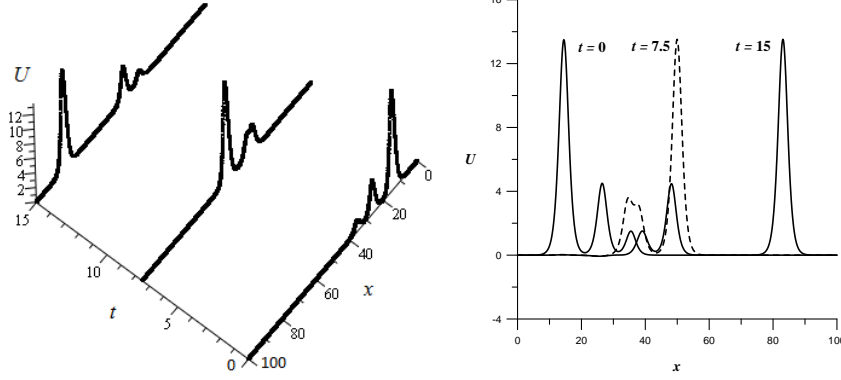


**Fig.10:** Interaction of three solitary waves    **Fig.11:** Interaction of three solitary waves

**Table 5**

Invariants for the interaction of two solitary waves at  $t = 15$ .

Method	$C_1$	$C_2$	$C_3$
Analytic	78	655.2	5450.4
Present	77.999994	655.069708	5451.895023
[10]	77.99539	652.8104	5411.639
[11]	78.00490	652.3474	5412.232
W(7,5)[22]	78.000004	655.263936	5451.005509

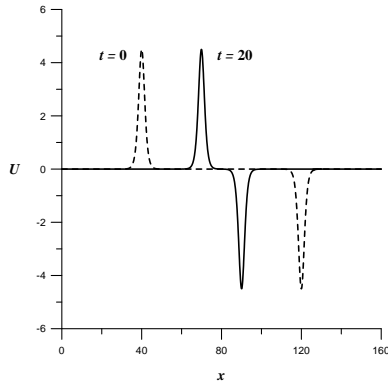
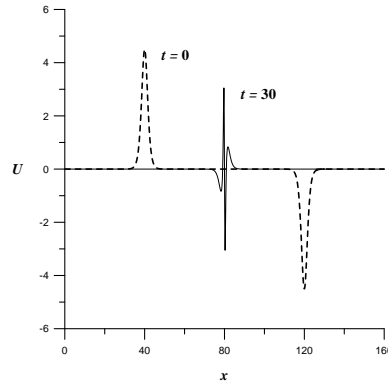
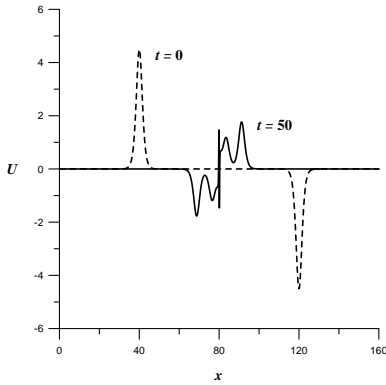
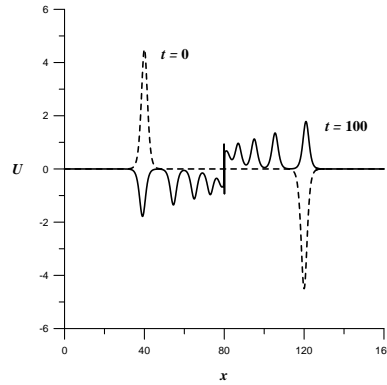
**3.4. Interaction of opposite waves.** The last interaction example is the interaction between two opposite waves that have exactly the same form but different signs. This case is relatively less considered problem in the literature. Although it is stated in [22] that the colliding solitons has never been treated before, it was also studied in [4] and [11].

The initial condition for colliding waves that are initially centered at  $x = 40$  and  $x = 120$  is given in [4] as

$$u_0(x) = 4.5\text{sech}^2[(x - 40)/2] - 4.5\text{sech}^2[(x - 120)/2]$$

which is also considered here with  $h = 0.1$  and  $k = 0.1$ .

These two opposite waves move towards each other and then a singularity occurs when they meet. The colliding yields trains of smaller waves on both sides, while the singularity gradually vanishes over time, see Figs.12-15.


**Fig.12:** Waves move towards each other

**Fig.13:** Colliding solitons with singularity

**Fig.14:** Singularity vanishes over time

**Fig.15:** Trains of smaller waves

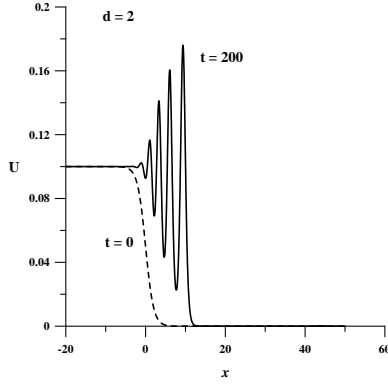
3.5. **Wave undulation.** Development of an undular bore is studied here by the initial function

$$u_0(x) = \frac{U_0}{2} \left( 1 - \tanh \left( \frac{x - x_c}{d} \right) \right)$$

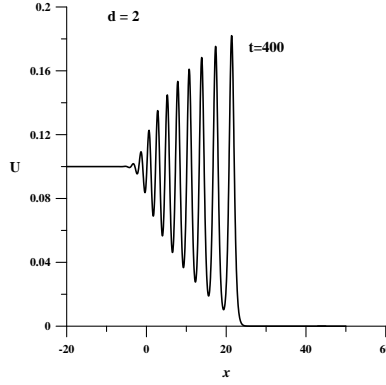
where  $d$  shows the slope between the still and deeper water and  $x_c$  is the center of the change in water level of magnitude  $U_0$ . The EW equation has not an analytical solution with the mentioned initial condition. So, only the invariants of the EW equation are considered in order to see the efficiency of the method. A comparison on invariants, position and amplitude of the leading undulation is presented in Table 6.

**Table 6**  
Development of undular bore

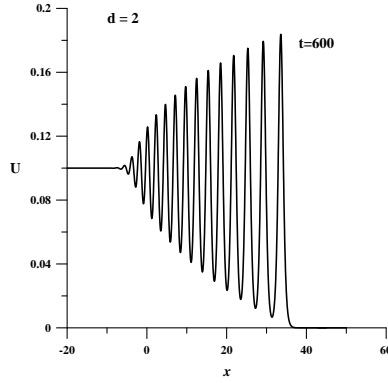
	Time	$C_1$	$C_2$	$C_3$	$x$	$U$
$d = 2$	0	2.0000000	0.19027759	0.018500000		
	200	3.0000000	0.32337149	0.033500252	9.4	0.17579731
	400	4.0000000	0.45637134	0.048500614	21.4	0.18142204
	600	5.0000000	0.58937051	0.063500976	33.6	0.18321870
	800	5.9999778	0.72236947	0.078501338	45.8	0.18383578
QBGM[14]	800	0.6002474	0.72386	0.078525	45.85	0.18471
DQM[14]	800	0.6025073	0.72402	0.07853	45.85	0.184713
$d = 5$	0	2.0000839	0.17512787	0.01625251521		
	200	3.0000815	0.30837385	0.03125247301	8.8	0.16035721
	400	4.0000815	0.44138580	0.04625256015	20.4	0.17905369
	600	5.0000815	0.57438765	0.06125265022	32.5	0.18242416
	800	6.0000801	0.70738790	0.07625274062	44.7	0.18364070
QBGM[14]	800	6.002578	0.708710	0.076277	44.75	0.18405
DQM[14]	800	6.025306	0.711361	0.076579	44.75	0.17259



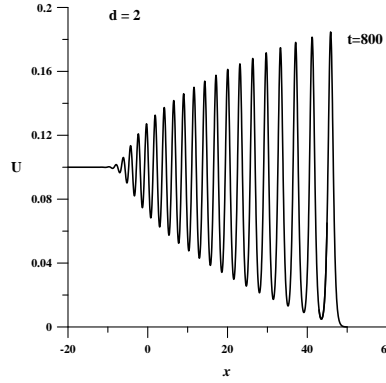
**Fig.16:** Undulation for  $d = 2$



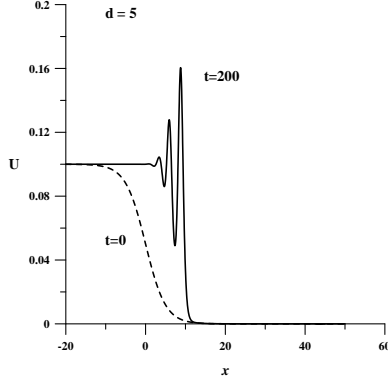
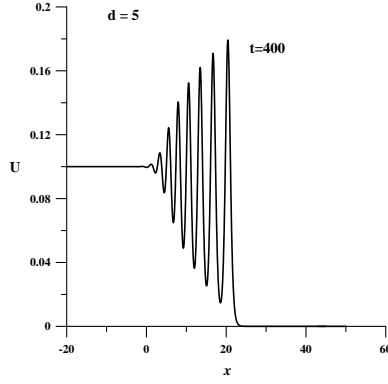
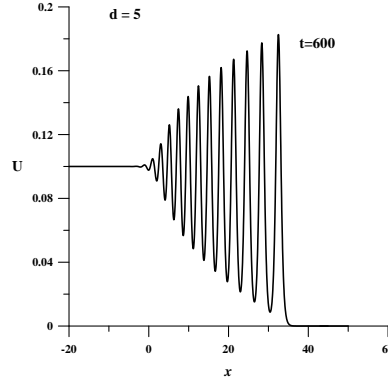
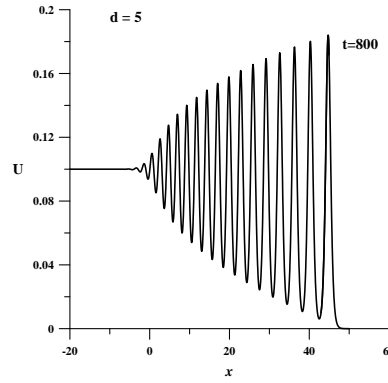
**Fig.17:** Undulation for  $d = 2$



**Fig.18:** Undulation for  $d = 2$



**Fig.19:** Undulation for  $d = 2$


**Fig.20:** Undulation for  $d = 5$ 

**Fig.21:** Undulation for  $d = 5$ 

**Fig.22:** Undulation for  $d = 5$ 

**Fig.23:** Undulation for  $d = 5$ 

Variations in invariants that are given in Table 7 are calculated numerically with the formula

$$M_i = \frac{C_i(\text{at time } t = 800) - C_i(\text{at time } t = 0)}{\text{Running time}}$$

and analytically with

$$\begin{aligned} M_1 &= \frac{dC_1}{dt} = \frac{d}{dt} \int_{x_0}^{x_N} u dx = \frac{1}{2} U_0^2 = 5 \times 10^{-3} \\ M_2 &= \frac{dC_2}{dt} = \frac{d}{dt} \int_{x_0}^{x_N} (u^2 + \mu u_x^2) dx = \frac{2}{3} U_0^3 = 6.66667 \times 10^{-4} \\ M_3 &= \frac{dC_3}{dt} = \frac{d}{dt} \int_{x_0}^{x_N} u^3 dx = \frac{3}{4} U_0^4 = 7.5 \times 10^{-5} \end{aligned}$$

The undulation profiles are illustrated in Figs.16-19 for  $d = 2$  and Figs.20-23 for  $d = 5$ .

**Table 7**

Variations in invariants				
	Method	$M_1 \times 10^{-3}$	$M_2 \times 10^{-4}$	$M_3 \times 10^{-5}$
$d = 2$	Analytical	5	6.66667	7.5
	Present	4.9999723	6.6511485	7.500167
	QBGM[14]	4.99997	6.66665	7.5
	DQM[14]	5	6.669387	7.507
	MM[14]	5	6.669387	7.507
	W(7,5)[22]	4.99937586	6.66667317	7.50000017
$d = 5$	Present	4.9999953	6.6532503	7.5001382
	QBGM[14]	4.99999	6.66665	7.7
	DQM[14]	5	6.671688	7.509
	MM[14]	5	6.671688	7.509

**3.6. The Maxwell wave.** The last problem for testing our method is the Maxwell wave where the starting function is

$$u_0(x) = 0.05 \exp\left(-\frac{(x-20)^2}{25}\right).$$

Again the analytical solution does not exist with this initial condition. The solutions are computed over  $\Omega = [0, 50]$  until  $T = 1000$ . The wave profiles are drawn in Figs.24-25 at four different times to figure out the behavior of the initial wave over time.

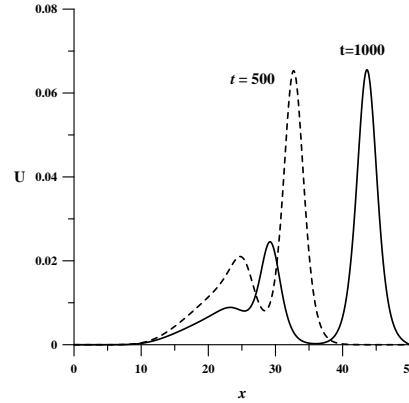
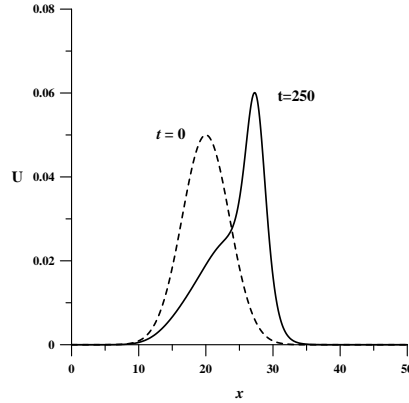


**Fig.24:** Wave profiles at  $t = 0$  and 250 **Fig.25:** Wave profiles at  $t = 500$  and 1000

There are some changes in the initial profile in course of time. It turns into a train such that while its amplitude becomes larger, the wave length becomes smaller and there are tails that will turn to a new small wave.

The invariants are presented at some different times in Table 8. The results show that the method is very conservative in this problem.

**Table 8**  
Invariants for the Maxwell wave

Time	C <sub>1</sub>	C <sub>2</sub>	C <sub>3</sub>
0	0.44311346	0.016292833	0.00063957919
100	0.44311348	0.016292567	0.00063957921
200	0.44311349	0.016291320	0.00063957928
300	0.44311349	0.016289148	0.00063957937
400	0.44311350	0.016287762	0.00063957944
500	0.44311349	0.016287480	0.00063957947
600	0.44311337	0.016287483	0.00063957947
700	0.44311225	0.016287440	0.00063957948
800	0.44310227	0.016287342	0.00063957947
900	0.44301341	0.016287228	0.00063957915
1000	0.44222656	0.016287133	0.00063955380

#### 4. CONCLUSION

In this study, cubic nonpolynomial spline based numerical method is implemented in order to get the solution of the EW equation. Over the uniform mesh, Crank-Nicolson formulas are employed for time discretization whereas Rubin and Graves[1] technique is used for the linearization. According to pointwise rate of convergence, the present method has second order accuracy for both space and time. Also the von-Neumann stability analysis shows that the proposed method is unconditionally stable. Six problems that related to single solitary wave, interaction of two, three and opposite solitary, the undulation bore and the Maxwell wave are examined for testing the numerical scheme. Comparisons between the obtained results and some earlier papers show that the present results are all acceptable and in agreement with those in the literature. Simple adaptation and yielding band matrices can be stated as the advantages of the method. On the other hand, according to your problem, requiring the determination of two parameters ( $\alpha$  and  $\beta$ ) is an undesirable situation. In conclusion, cubic nonpolynomial spline method can be considered as a conservative numerical method that leads to reasonable results.

#### REFERENCES

- [1] Rubin S.G. and Graves R.A., Cubic spline approximation for problems in fluid mechanics, Nasa TR R-436, Washington, DC, (1975).
- [2] Morrison P.J., Meiss J.D., Carey J.R., Scattering of RLW solitary waves, Physica 11D (1981) 324–36.
- [3] Gardner L.R.T., Gardner G.A., Solitary waves of the equal width wave equation, J Comput Phys 101 (1992) 218–23.
- [4] Garcia-Archilla B., A spectral method for the equal width equation, J Comput Phys 125 (1996) 395–402.
- [5] Zaki S.I., A least-squares finite element scheme for the EW equation, Comput Meth Appl Mech Eng 189 (2000) 587–94.
- [6] Saka B., Dag I., Dogan A., A Galerkin method for the numerical solution of the RLW equation using quadratic B-splines, Int J Comput Math 81 (2004) 727–739.
- [7] Dag I., Saka B., A cubic B-spline collocation method for the EW equation. Math Comput Appl 9 (2004) 381–392.

- [8] Dogan A., Application of Galerkin's method to equal width wave equation. *Appl Math Comput* 160 (2005;) 65–76.
- [9] Esen A., A numerical solution of the equal width wave equation by a lumped Galerkin method, *Appl Math Comput* 168 (2005) 270–282.
- [10] Raslan K.R., Collocation method using quartic B-spline for the equal width (EW) equation, *Int J Comput Math* 81 (2004) 63–72.
- [11] Raslan K.R., A computational method for the equal width equation, *Appl Math Comput* 168 (2005) 795–805.
- [12] Ramos J.I., Explicit finite difference methods for the EW and RLW equations, *Appl Math Comput* 179 (2006) 622–638.
- [13] Ramos J.I., Solitary waves of the EW and RLW equations, *Chaos Solitons and Fractals* 34 (2007) 1498–1518.
- [14] Saka B., Dag I., Dereli Y., Korkmaz A., Three different methods for numerical solution of the EW equation, *Engineering Analysis with Boundary Elements* 32 (2008) 556–566.
- [15] Rashidinia J., Mohammadi R., Non-polynomial cubic spline methods for the solution of parabolic equations, *Int. J. Comput. Math.* 85:5 (2008) 843–850.
- [16] Griewanka A., El-Danaf T.S., Efficient accurate numerical treatment of the modified Burgers' equation, *Applicable Analysis* 88 (2009) 75–87.
- [17] Rashidinia, J., Mohammadi, R.: Tension spline approach for the numerical solution of non-linear Klein-Gordon equation, *Comput. Phys. Commun.* 181 (2010) 78–91.
- [18] Jalilian, R.: Non-polynomial spline method for solving Bratu's problem, *Comput. Phys. Commun.* 181 (2010) 1868–1872.
- [19] Roshan T., A Petrov–Galerkin method for equal width equation, *Applied Mathematics and Computation* 218 (2011) 2730–2739.
- [20] El-Danaf T.S., Ramadan M.A., Abd Alaal F.E.I, Numerical studies of the cubic non-linear Schrödinger equation, *Nonlinear Dyn.* 67 (2012) 619–627.
- [21] Chegini N.G., Salaripanah A., Mokhtari R., Isvand D., Numerical solution of the regularized long wave equation using nonpolynomial splines, *Nonlinear Dyn.* 69 (2012) 459–471.
- [22] Dereli Y., Schaback R., The meshless kernel-based method of lines for solving the equal width equation, *Applied Mathematics and Computation* 219 (2013) 5224–5232.

DEPARTMENT OF MATHEMATICS, AKSARAY UNIVERSITY, 68100, AKSARAY, TURKEY.  
*E-mail address:* [asahinhc@gmail.com](mailto:asahinhc@gmail.com)